

Low-Cost Dual-Band Circularly Polarized Switched-Beam Array for Global Navigation Satellite System

M. Maqsood, S. Gao, *Member, IEEE*, T. Brown, *Member, IEEE*, M. Unwin, R. de vos Van Steenwijk, J. D. Xu and C. I. Underwood

Abstract— This paper presents the design and development of a dual-band switched-beam microstrip array for Global Navigation Satellite System (GNSS) applications such as ocean reflectometry and remote sensing. In contrast to the traditional Butler matrix, a simple, low cost, broadband and low insertion loss beam switching feed network is proposed, designed and integrated with a dual band antenna array to achieve continuous beam coverage of $\pm 25^\circ$ around the boresight at the L1 (1.575 GHz) and L2 (1.227 GHz) bands. To reduce the cost, microstrip lines and PIN diode based switches are employed. The proposed switched beam network is then integrated with dual-band step-shortened annular ring (S-SAR) antenna elements in order to produce a fully integrated compact-sized switched beam array. Antenna simulation results show that the switched beam array achieves a maximum gain of 12 dBic at the L1 band and 10 dBic at the L2 band. In order to validate the concept, a scaled down prototype of the simulated design is fabricated and measured. The prototype operates at twice of the original design frequency i.e. 3.15 GHz and 2.454 GHz and the measured results confirm that the integrated array achieves beam switching and good performance at both bands.

Index Terms—Antenna, antenna array, global positioning system, GPS, shorted annular ring antenna, switched beam antenna

I. INTRODUCTION

CIRCULARLY polarized antenna arrays are useful in numerous applications such as GNSS remote sensing, surveillance, interference mitigation, and satellite communications particularly at L and S bands [1-7]. Apart from offering high gain, an antenna array can also achieve beam switching and/or scanning capability by changing the relative phase difference between individual elements. Moreover, enabling the antenna array to operate at two or more frequency bands simultaneously has numerous benefits; the antenna can be used for more than one application at the same time, signal to noise ratio (S/N) can be improved through

frequency diversity, measurement accuracy can be improved through differential measurements and system (effective) bandwidth can be increased by receiving the signal at more than one frequency [8-9]. Therefore combining the benefits of multiple frequency operation along with switched beam capability can result in a very attractive antenna for small satellites.

GNSS remote sensing applications like ocean reflectometry use the L-band navigation signals already being transmitted by GPS (Global Positioning System), GLONASS (Global Navigation Satellite System) and Galileo systems for estimating the wind speed and direction of ocean currents [1]. The high gain antenna array onboard the satellite picks up GNSS signals reflected by the ocean surface and processes them for the corresponding measurements. The antenna beam is usually directed away from the Nadir direction in order to increase the visibility of the reflected signals. Moreover, availability of the L2 GNSS signal for civilian use (L2C) has allowed data collection at more than one frequency which helps to improve accuracy and determine the ionospheric effects through differential measurements. Some work on antennas for GNSS reflectometry has been carried out in the past but most of the reported antennas have either fixed beams or high cost [1-3]. For GNSS reflectometry using small satellites, it is necessary to have a circularly polarized array antenna which can have a high gain, dual band capability and electronic beam steering capability keeping both the cost power consumption low. The main purpose of this work is to bridge this gap.

Circularly polarized antenna arrays are also a major candidate for GNSS anti-jamming and interference mitigation applications. A variety of techniques such as null steering, beam switching, adaptive polarisation etc. have been developed over the past two decades that use phased array antennas to suppress the incoming interference and jamming signals [5-6].

Although the beam switching / scanning capability of phased array antennas (adaptive and non-adaptive) have successfully been used both commercially and in the military, their operation requires complex electronics packages and expensive phase shifters which usually result in a high cost antenna with high power consumption [10-11].

A simple technique that can reduce the cost of control electronics while keeping the high gain functionality of the beam steering antenna replaces the expensive phase shifters

Manuscript received April 29, 2013.

M. Maqsood was with Surrey Space Centre and is now with Institute of Space Technology, Pakistan (e-mail: moazammaqsood@hotmail.com).

S. Gao was with Surrey Space Centre and is now at the University of Kent, UK (email: s.gao@kent.ac.uk).

T. Brown and C. I. Underwood are with University of Surrey, UK.

M. Unwin and R. de vos van Steenwijk are with Surrey Satellite Technology Ltd., UK.

J. D. Xu is with Northwestern Polytechnical University, P.R. China.

with simple switching mechanism to point the antenna beam into different directions. The resulting antenna is called a switched beam antenna array and is able to direct the antenna beam to different directions based on the selection input. Similar to a beam scanning antenna, a switched beam antenna provides continuous coverage across the boresight while keeping the antenna manufacturing cost as well as the power consumption very low.

This paper presents the design of a circularly polarized dual-band switched-beam antenna array for GNSS reflectometry applications. The antenna design is a 4 element linear array incorporating a broadband switching mechanism in order to provide continuous coverage for $\pm 25^\circ$ around the boresight. Since GNSS signals change their polarization to left hand circular after reflecting from the surface of the ocean, the proposed antenna array is designed to receive left hand circular polarized (LHCP) signals. Antenna simulation results show that the array achieves a maximum boresight gain of 12 dBic at the L1 band while 10 dBic at the L2 band. The major contributions of this work are given below:

(a) Design and development of a broad band beam switching feed network. The proposed design has demonstrated 26.82% operational bandwidth.

(b) Design, development and manufacturing of a fully integrated dual-band switched-beam antenna array. In contrast to the previously reported designs [13-14], the proposed antenna array offers; higher gain at multiple frequencies, beam switching along the array axis and low manufacturing cost.

Section II of the paper briefly introduces some common switching techniques used for switched-beam antennas. Section III presents the design of a broadband switching network while section IV briefly presents the design of the step shorted annular ring (S-SAR) antenna element. Section V describes the design of the antenna array while section VI explains the prototype manufacturing and discusses measurement results. Section VII concludes the paper.

II. BEAM SWITCHING TECHNIQUES

Several feed network designs have been presented in the literature that can provide switched beam capability for antenna arrays [10-13]. The presented designs have certain advantages and disadvantages over one another and thus can be selected with respect to the application of interest.

A. Butler Matrix

The Butler matrix has been the most commonly used beam switching feed network for antenna arrays since it was first described in [10]. It is a microwave beam switching network that usually consists of N inputs and N outputs ($N = 2^n$) and can be implemented using waveguides or microstrip transmission lines. A Butler matrix uses hybrid couplers to achieve equal amplitude and a progressive phase distribution across different output ports. The phase difference between each port is constant for any selected input and its value decides the squint direction of the antenna beam.

Although the Butler matrix is able to provide precise amplitude and phase distribution across the N outputs, there

are some design factors to be considered. Firstly, the Butler matrix uses branchline couplers as the basic building blocks increasing the size of the feed network enormously. Secondly, the implementation of the planar Butler matrix requires a cross over. The cross over can be implemented using a through via connection but requires a lot of care in design and manufacturing due to associated parasitic inductance and the fact that the cross over path may touch the antenna element. A zero degree hybrid [12-13] can avoid the unwanted cross over but only at the cost of further increasing the feed network size.

B. Single Pole Multiple Throw (SPMT) switch

A SPMT microwave switch based feed network is presented in [14]. The feed network is designed to switch the main beam of a single band antenna array for a continuous coverage. The output of the SPMT switch is connected to the rest of the feed network at one of the four equal length input feed lines where each input line results in a different beam direction while the rest of the three input lines are left open ended. The $\lambda_g/2$ length of the open ended transmission lines reflects this open circuit at the feed joint stopping any backward power flow (from feed network into the switch). However, this approach limits the operational bandwidth of the feed network which is only 120 MHz (6.66% at 1.8 GHz) as presented in [14].

Comparing the Butler matrix and the SPMT switch for beam switching, it can be observed that the Butler matrix can operate with a wider bandwidth by employing broadband branchline couplers but its disadvantage is the large area consumption where as the SPMT switch presented in [14] has a compact size but limited bandwidth. Another potential disadvantage of the Butler matrix is fixed switching directions which may not give a continuous coverage for a sharp beam.

C. Proposed broadband beam switching method

This paper presents an innovative yet simple technique in order to achieve switching capability for a wider bandwidth (0.8 GHz to 1.9 GHz) with greater than 15 dB isolation between switching branches. The proposed technique use PIN diodes to provide an open or short circuit at the point of contact. Careful selection of PIN diodes can provide minimum insertion loss while keeping the overall antenna size small and low cost. Fig. 1 presents the simulation layout of a small feed network demonstrating the isolation of PIN diode.

The simulation layout shows three input ports (labelled as port 1, port 2 and port 3) and two output ports (labelled as output 1 and output 2). Port 1 is the primary input while port 2 and port 3 are the switching legs to be selected for a desired beam direction. In the absence of ports 2 (switch leg 1) and 3 (switch leg 2), the input from port 1 should split and be transmitted equally to output 1 and output 2. However, in the presence of switch leg 1 and switch leg 2, the input power may not equally transmit to output 1 and output 2 as some power will flow towards switch leg 1 and switch leg 2. In order to stop the incoming energy switch leg 1 uses a $\lambda_g/2$ long open ended transmission line (similar to [14]) while switch leg 2 uses a shorter line connected through (a reverse biased) PIN diode. Simulation result presented in Fig. 2 compares the isolation of switch leg 1 (port 2) and switch leg 2 (port 3) with

the input (port 1). It can be seen from the comparison that the switch leg 2 using a PIN diode stops the incoming energy more efficiently providing better isolation.

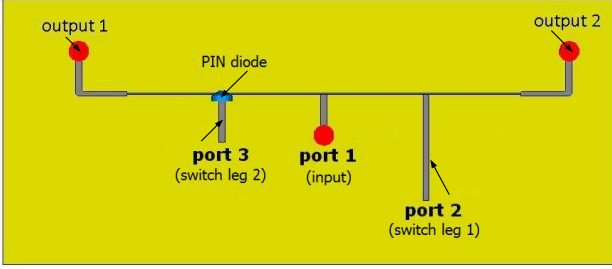


Fig. 1. Simulation layout of switch feed isolation test.

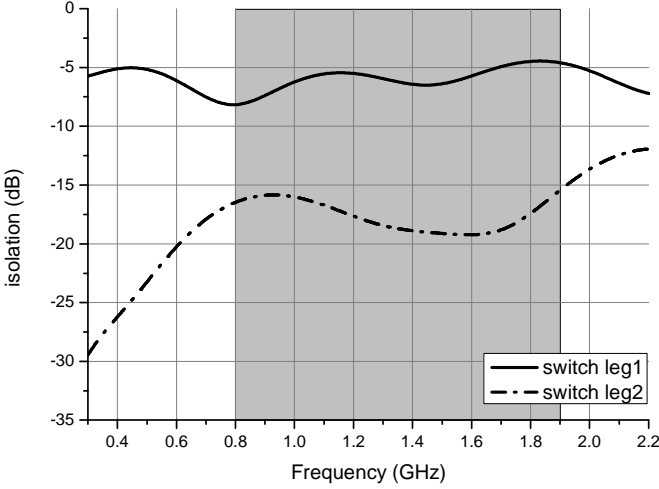


Fig. 2. Simulation comparison of PIN diode isolation with $\lambda_g/2$ open ended transmission line

III. A BROADBAND SWITCHED BEAM FEED NETWORK

This paper presents the design of a broadband beam switching feed network for a circularly polarized antenna array. In contrast to the traditional Butler matrix, the proposed feed network consumes less physical space and offers more than 25% operational bandwidth (700 MHz at 2.8 GHz). The compact size of the feed network is achieved by avoiding the un-necessary branch line couplers that are the basic building blocks of the Butler matrix. Further size reduction can be achieved by choosing a high permittivity substrate but the overall antenna size is limited by the inter-element spacing. Another advantage of the proposed feed network design is the use of reverse biased PIN diodes to stop backward power flow. This improves isolation between switching branches at multiple frequencies. The design of the proposed beam switching network is described in detail below: First, a simple feed network design providing a 6 dB power split is presented. The design of a PIN diode based switch and its integration with the basic feed network is presented afterwards.

A. Basic Design

A corporate type 1 to 4 power splitter is used as the basic design for the feed network. A single 50Ω input transmission line is split into two 100Ω lines to achieve equal power split.

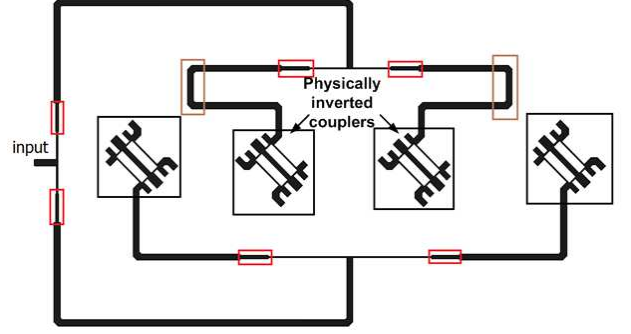


Fig. 3. Basic 1 x 4 power split feed network.

Each 100Ω section is transformed back to 50Ω transmission line by using an impedance matching quarter wavelength transformer (marked by red boxes). The same sequence is applied again in order to achieve further power split. Each of the four branches are then connected to a broadband compact branch line coupler (marked by black boxes) in order to achieve circular polarization at multiple frequencies. Fig. 3 shows the simulation layout of the basic feed network. It is worth mentioning that two of the four hybrid branch line couplers are physically inverted and thus 180° phase compensation should be provided in order to achieve maximum gain in the required direction. This is achieved by adjusting the line length of the top (feed) part (shown with brown boxes).

B. Broadband PIN switch

The next task was to employ a switching mechanism ensuring an appropriate phase difference between consecutive branches for multiple switching states. Two such switches, one at the top and the other at the bottom of the feed network vary the phase difference between the four antenna elements. In contrast to the SPMT switch design in [14], the proposed beam switching network uses small microstrip lines with PIN diodes to achieve the appropriate phase difference between antenna elements and to achieve better isolation between the switching legs. Careful selection of PIN diodes can minimize insertion loss while keeping the overall antenna size small and low cost.

Fig. 4 presents the schematic layout of the PIN diode based switch where the highlighted path shows the transmission of the incoming signal for a positive biasing voltage at B1, B2 and B3. Quarter wavelength long lines along with RF choke inductors (100 nH) have been used to isolate the RF energy and DC supply. Further protection is achieved by using shunt capacitors ($10\mu\text{F}$) at all the biasing points. The series resistance of the RF choke inductors helps in limiting the flow of current. The PIN diode package used for implementing the switching circuit is BAP50-03 [15] by NXP semiconductors. The selection of the PIN diode is based upon the value of the reverse biased capacitance and forward biased insertion loss. The operation of the switch is very simple. Correct biasing ($\pm 5\text{V}$, 40 mA) at the corresponding biasing points put the required PIN diodes in forward bias configuration allowing the RF energy to transmit from the input to one of the four switching branches (state 1 to 4). Similarly the PIN diodes are

put in the reverse biased configuration stop the flow of RF energy through them creating an open circuit.

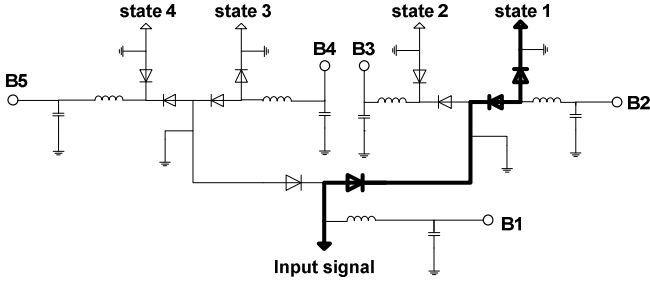


Fig. 4. Feed network layout of PIN diode switch (quarter wave lines not shown).

IV. ANTENNA ELEMENT FOR THE SWITCHED BEAM ARRAY

The antenna element used for the switched beam array is the dual-band step-shortened annular ring (S-SAR) antenna [16]. A shorted annular ring antenna element is used as it is well known for its capability to minimize the surface and lateral wave propagation [17]. Although such an antenna element can reduce the coupling between the array elements, appropriate separation between the antenna elements will still be required to ensure high boresight gain and avoid grating lobes.

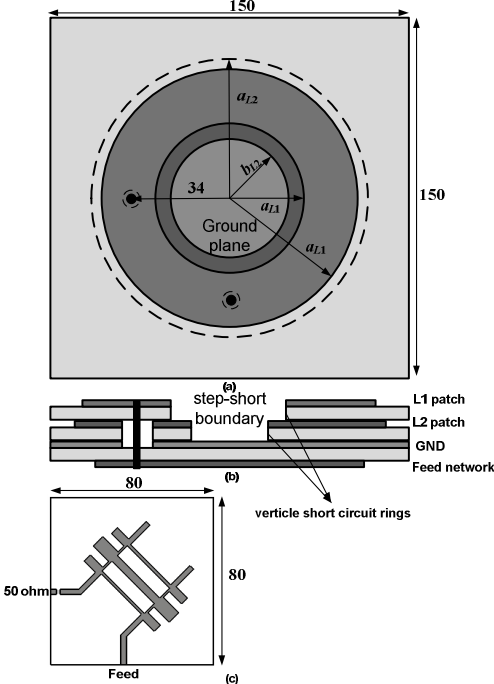


Fig. 5. (a) Top (b) side and (c) bottom view of the novel dual band step-shortened annular ring (S-SAR) antenna

The antenna design configuration and its performance are presented in [16]. However, a brief description of the antenna operation is presented here for the sake of completeness. The antenna configuration is presented in Fig. 5 with all the design variables clearly written. The antenna element consists of two shorted circular annular ring elements stacked together. The top element resonates at the L1 band while the bottom element resonates at the L2 band. The two most important dimensions of the annular ring antenna are the internal and external radii

of the annular ring. The external radius of the ring (referred to as a) controls the antenna directivity and is selected to satisfy the condition of zero lateral and surface wave propagation [17]. On the other hand the inner boundary (referred to as b), needs to be shorted to the ground and its value determines the resonant frequency. Therefore, these two elements result in two different set of design values ($a_{L1}=52.8$ mm, $b_{L1}=23.8$ mm and $a_{L2}=55$ mm, $b_{L2}=16.5$ mm) for dual-band operation. Firstly, the inner ring of the bottom element is connected to the ground. This connection extends the ground plane to the body of the bottom ring. The inner ring of the top element is then connected directly to the bottom ring body. Circular polarization is achieved by using a compact broadband branch line hybrid coupler integrated with the antenna. The performance of the compact broadband branch line coupler is presented in [18] providing 3 dB power split and 90° phase difference for more than 28% bandwidth.

V. DESIGN OF INTEGRATED ARRAY ANTENNA AND SIMULATION RESULTS

In order to explain the operating principle and beam switching mechanism of the proposed switched beam antenna, the simulation layout of the feed network is presented in Fig. 6. The DC biasing circuit is removed to give more clarity while the PIN diode locations are represented by small gaps.

A. Beam switching mechanism

The beam switching mechanism of the proposed feed network can be explained by considering the standalone antenna elements as the point sources [19]. The phase advancement or retardation between the E fields of n number of point sources (on the same line) of equal amplitude and arbitrary phase difference is given as:

$$\psi = d_r \cos \varphi + \delta \quad (1)$$

where φ is angle between the array axis and any arbitrary direction and d_r is the distance between the sources expressed in radians; that is $d_r = 2\pi d/\lambda$ while δ is the relative phase difference between consecutive sources.

According to [19] the E-field maximum is in the direction of φ when ψ is zero. Putting $\psi = 0$ in (1) leads to (2):

$$\varphi = \cos^{-1} \left(-\frac{\delta}{d_r} \right) \quad (2)$$

which means that for a fixed array spacing, the antenna beam can be switched in different directions for a selection of δ or vice-versa.

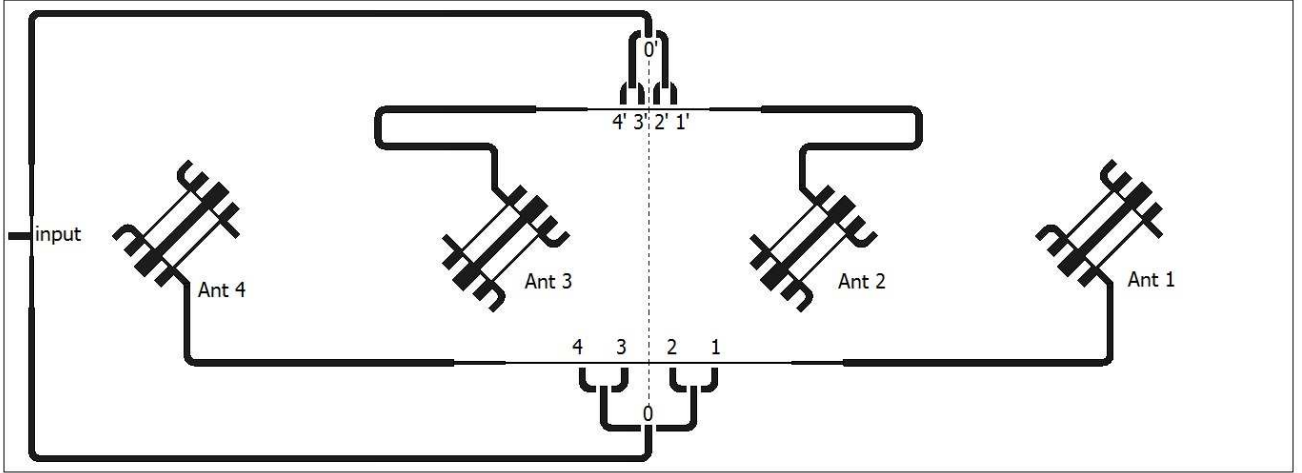


Fig. 6. Simulation layout of the switched beam antenna feed network (without DC biasing)

B. Mapping of required beam direction to the switch position

The required beam switching directions (φ_n) are calculated in order to provide a continuous coverage across boresight. Equation (2) is used to calculate the required relative phase difference (δ_n) between the antenna elements.

The calculated phase difference is converted to physical distance between the antenna elements (using equation 3) thereby resulting in the selection points 1, 1'; 2, 2'; 3, 3' and 4, 4' (of Fig. 6).

$$\delta_{dist} = \frac{2\pi |d_{\delta_n}|}{\lambda_g} \quad (3)$$

where λ_g is the guided wavelength.

Due to the requirement of symmetric coverage, the same configuration has been used on both the right and left hand sides of the 00' reference line. Table I presents the required beam switching directions and the respective positions of the switching lines.

TABLE I
BEAM DIRECTION MAPPING TO RESPECTIVE SWITCH POSITIONS

Beam direction	Relative phase difference (δ)	Relative phase to distance conversion ($d_{\delta} = \text{mm}$)	Required switch and distance from 00' (mm)	
-20°	+86.18°	+12	1	18
			1'	6
-10°	+43.75°	+6	2	9
			2'	3
+10°	-43.75°	-6	3	-9
			3'	-3
+20°	-86.18°	-12	4	-18
			4'	-6

It is worth mentioning here that the required beam direction presented in Table I is the complementary angle to φ (used in equation 1) and is calculated across the array axis. Moreover, the corresponding values of relative phase difference are evaluated with respect to the center frequency of 1.4 GHz.

Fig. 7 presents the simulation results of relative amplitude and phase difference between consecutive antenna elements. The results have been presented for the PIN switch connecting

at points 11' (Ref. to Fig. 6). It has to be noted that the transmission coefficients s_{21} to s_{51} (in Fig. 7) are referred to the antennas 1 to 4 (in Fig. 6) whereas s_{11} refers to the input port. It can be seen that the magnitude of the reflection coefficient remains less than -10 dB while 6 dB power split can be observed between the consecutive ports.

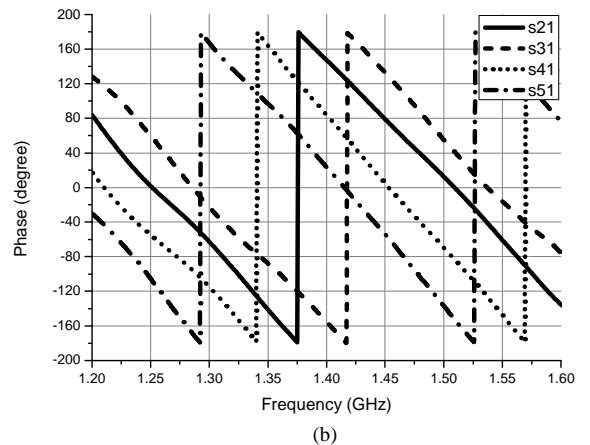
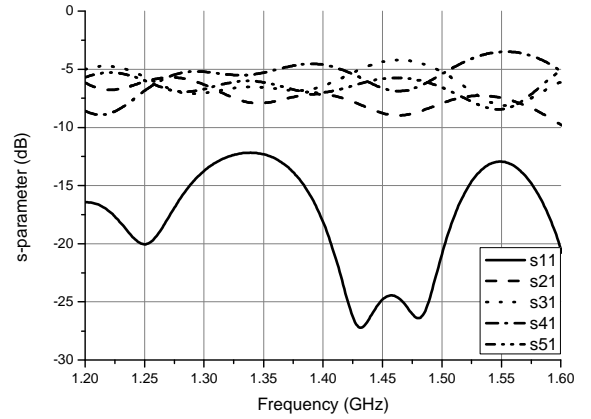


Fig. 7. (a) Simulated s-parameter amplitude and (b) phase response of the proposed feed network for -20° switching state.

A strong dip in $|s_{11}|$ can be observed at 1.45 GHz indicating the design frequency of the feed network (approximately at the center of L2 and L1 bands). Nearly equal phase differences can also be observed at the consecutive feed ports at both

frequencies. However, it can be observed from Fig. 7(a) that the transmission magnitudes are not stable (better than 5 dB) with frequency especially at the L1 band. This variation is due to the several bends in the transmission line network. Another factor that can be responsible for this variation is due to some parts of the feed network run in very close proximity thereby producing some resonance effect near the L1 band. This is further verified from the simulation presented in Fig. 8 where s_{21} transmission coefficient has been plotted for different feed network scenarios.

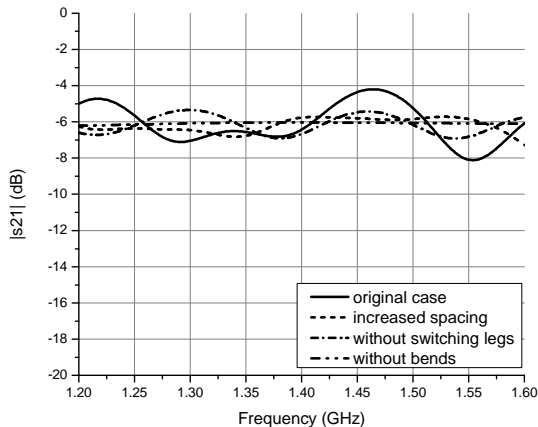


Fig. 8 Simulated transmission coefficients ($|s_{21}|$) of different feed network scenarios

VI. ANTENNA MANUFACTURING AND MEASUREMENT RESULTS

A. Antenna fabrication

In order to validate the beam switching capability of the proposed broadband feed network a scaled down prototype of the antenna array was fabricated. A scaling factor of $\frac{1}{2}$ was selected to bring the antenna size within the limits of available fabrication facilities. The scaled down prototype now operates at 3.15 GHz and 2.454 GHz (twice that of the L1 and the L2 bands). In order for the scaled prototype to achieve the same switching directions the distance of the switching legs from the feed center was decreased. The inter-element spacing was kept at 0.7λ (75 mm at 2.8 GHz). The four element antenna array resulted in an overall size of 600 mm x 230 mm.

Duroid 5880 ($\epsilon_r = 2.2$, $h = 1.575$ mm) was used to manufacture the annular ring elements while the feed network was fabricated using FR4 epoxy ($\epsilon_r = 4.55$, $h = 1.6$ mm). Once fabricated, holes were drilled in the substrate to make annular rings. Residual substrate was cut out using a hand knife. Thin strips of copper were hand soldered on the inner boundaries to connect the annular rings to the ground. It is worth mentioning that human errors caused by manual cutting and soldering of the shorted annular rings can deform the antenna elements thereby shifting the resonant frequency as well as degrading the polarization purity.

Fig. 9 shows the front and backside of the manufactured antenna prototype. Nylon screws were used to fasten the antenna layers together. The four elements array antenna has an area of 300 mm x 75 mm while the feed network has a greater width to provide extra ground plane space for the top

and bottom switches. An external 180° degree hybrid was used to provide compensation for the physically inverted (middle) hybrid couplers. The two ports of the external hybrid were connected between the top and bottom SMA connectors marked in the red boxes. External wires were connected to the integrated antenna to provide 5V DC biasing voltage and 40 mA current to the PIN diodes.

B. Antenna measurement results

Antenna measurements were carried out in a local anechoic chamber. The chamber was calibrated from 2 GHz to 4 GHz. A broadband left hand circularly polarized conical spiral antenna was used as a transmitter while the antenna under test (AUT) was mounted at the receiving end on a 360° turntable. Different beam directions of the array antenna were selected by manually connecting the power supply to provide the correct biasing voltage and current. Antenna measurement results are presented in Fig. 9 to Fig. 12.

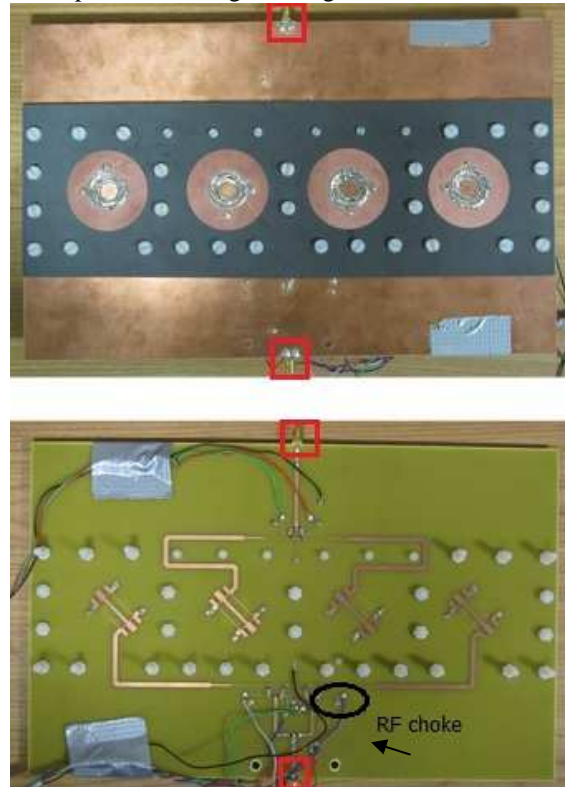


Fig. 9 Front and back side of switched beam antenna array

The reflection coefficient curves presented in Fig. 10 shows two distinct dips at 2.454 GHz and 3.2 GHz (near 3.15 GHz). Other distinct dips at 2.8 GHz and 3 GHz are due to the effect of the broadband branchline couplers and the external hybrid coupler respectively. The measured $|s_{11}|$ has been presented for all four switching states and shows consistency in the antenna performance. The simulated $|s_{11}|$ curve is not presented in Fig. 10 as the antenna simulation did not include the effect of external hybrid coupler.

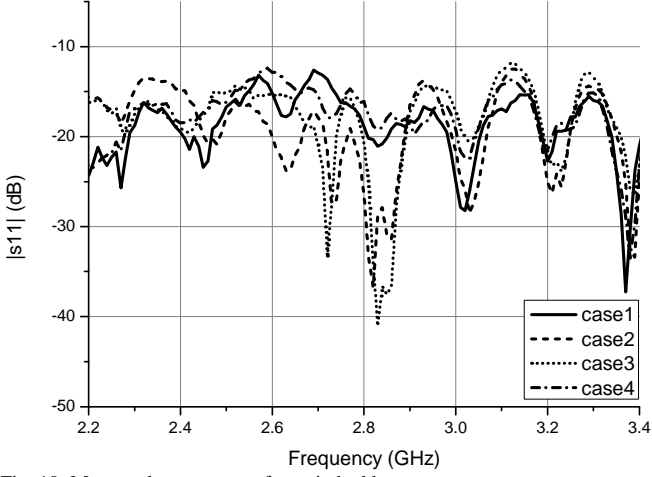


Fig. 10. Measured s_{11} response for switched beam array antenna.

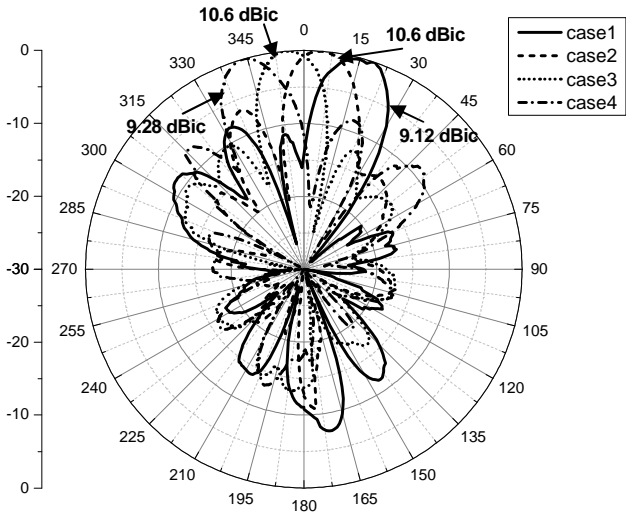


Fig. 11. Measured radiation pattern for switched beam array antenna at 2.454 GHz.

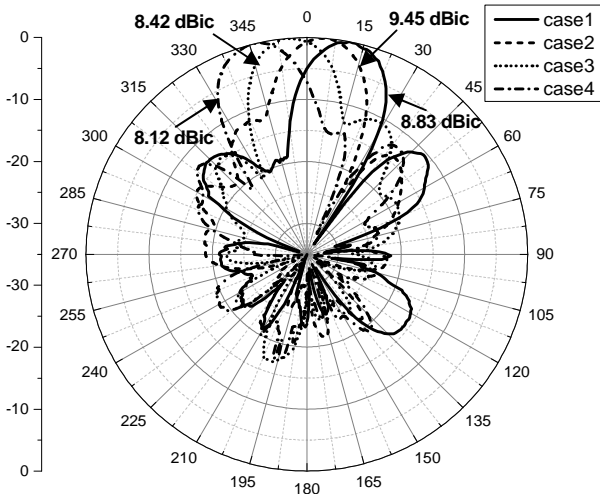


Fig. 12. Measured radiation pattern for switched beam array antenna at 3.15 GHz.

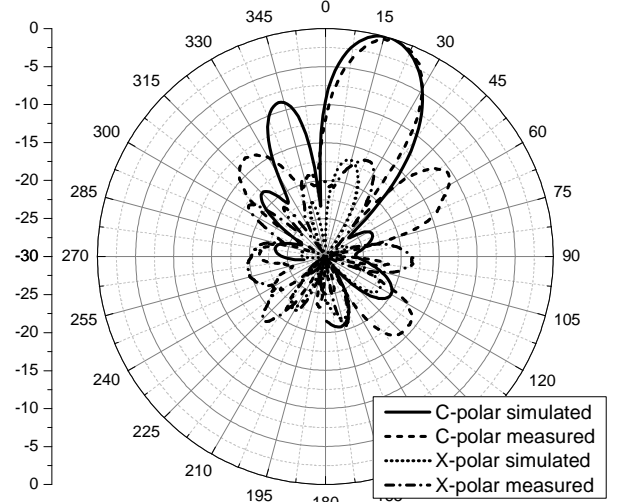


Fig. 13. Comparison of simulated and measured co-polar and cross-polar pattern for switched beam array antenna at 2.454 GHz.

The measured (normalized) radiation patterns of the array antenna presented in Fig. 11 and Fig. 12 show different beam switching directions. The antenna has a left handed circular polarization with a maximum gain of 9.45 dBic at 2.454 GHz and 10.8 dBic at 3.15 GHz. Fig. 13 compares the simulated and measured patterns of the array antenna at 2.454 GHz and shows close agreement between the co-polar and cross polar patterns. The antenna gain across the bandwidth of interest presented in Table II shows 40 MHz coverage at both bands. The accumulated 3 dB beam width of the array antenna across the boresight is 47° at 2.454 GHz (from -25° to $+22^\circ$) and 50° at 3.15 GHz (from -25° to $+25^\circ$).

TABLE II
SIMULATED AND MEASURED ANTENNA GAINS ACROSS 2.454 GHz AND 3.15 GHz

Frequency (GHz)	Gain (dBic) in different directions				
		Case1 (+20°)	Case2 (+10°)	Case3 (-10°)	Case4 (-20°)
2.434	Simulated	8.8	9.8	9.7	8.7
	Measured	8.53	8.83	8.09	7.70
2.454	Simulated	9.4	10.3	10.4	9.5
	Measured	8.83	9.45	8.42	8.12
2.474	Simulated	8.4	9.8	9.1	8.7
	Measured	8.74	9.52	8.84	8.32
3.13	Simulated	11.4	11.6	11.5	10.8
	Measured	7.49	8.73	9.50	7.92
3.15	Simulated	11.5	11.8	11.7	11.1
	Measured	9.12	10.6	10.6	9.28
3.17	Simulated	11.4	11.7	11.6	11.2
	Measured	8.97	10.6	10.6	8.53

VII. CONCLUSION

The design of a low cost dual-band switched beam circularly-polarized array antenna for GNSS reflectometry applications has been presented. The proposed antenna and the

integrated beam switching network use low cost PIN diodes in order to switch between four different beam directions. The beam switching and multiple frequency allows for higher resolution in remote sensing applications. In comparison to a previously reported SPMT switching technique, the use of PIN diodes enhances the operational bandwidth and also improves the isolation between switching legs. The simulation and measurement results show that the array antenna achieves above 9.4 dBic gain at 2.454 GHz and above 10.5 dBic at 3.15 GHz. The antenna is fabricated with space qualified material and can be easily mounted onboard small satellites. However, the final flight model may require integrating a small microcontroller unit to the antenna switching the required beam direction based on a single control input.

REFERENCES

- [1] M. Unwin, S. Gao, R. De Vos Van Steenwijk, P. Jales, M. Maqsood, C. Gommenginger, J. Rose, C. Mitchell and K. Partington, "Development of Low-Cost Spaceborne Multi-Frequency GNSS Receiver for Navigation and GNSS Remote Sensing", *International Journal of Space Science and Engineering*, Vol. 1, No. 1, pp 20-50 (Invited Paper)
- [2] M. Maqsood, B. Bhandari, S. Gao, R. D. Steenwijk and M. Unwin, "Development of Dual-Band Circularly Polarized Antennas for GNSS Remote Sensing onboard Small Satellites", *ESA Workshop on Antennas for Space Applications*, ESTEC, Netherlands, 2010
- [3] W. Imbraile, S. Gao and L. Boccia, *Space Antenna Handbook*, John Wiley & Sons, 2012
- [4] P. Rizki Akbar, J. Tetuko S. S. & H. Kuze (2010): A novel circularly polarized synthetic aperture radar (CP-SAR) system onboard a spaceborne platform, *International Journal of Remote Sensing*, 31:4, 1053-1060
- [5] Y. Jiang, H. Yang and X. Wang, "The Design and Simulation of an S-band Circularly Polarized Microstrip Antenna Array", *Progress in Electromagnetics Research Symposium Proceedings*, Xi'an, China, March 22-26, 2010
- [6] Casabona, M. M. and M. W. Rosen (1999). "Discussion of GPS Anti-Jam Technology." *GPS Solutions* 2(3): 18-23.
- [7] NovaSar-S brochure - Surrey Satellite Technology Ltd, Available: <http://www.sstl.co.uk/Downloads/SSTL-Brochure-pdfs/1904-SSTL-NovaSAR-Brochure>.
- [8] P. Kumar and N.Bisht, "Stacked Coupled Circular Microstrip Patch Antenna for Dual Band Applications", *Progress In Electromagnetics Research Symposium Proceedings*, Suzhou, China, Sept. 12-16, 2011.
- [9] Theodore S. Rappaport, "Wireless Communications: Principles and Practice", Prentice Hall, 1996
- [10] J. Butler, R. Lowe, "Beam-Forming Matrix Simplifies Design of Electronically Scanned Antennas", *Electronic Design*, volume 9, pp. 170-173, April 12, 1961.
- [11] Chia-Chan Chang; Ruey-Hsuan Lee; Ting-Yen Shih; , "Design of a Beam Switching/Steering Butler Matrix for Phased Array System," *Antennas and Propagation*, *IEEE Transactions on* , vol.58, no.2, pp.367-374, Feb. 2010
- [12] Thakare, A.P.; Shelke, R.N.; , "Planar implementation of Butler Matrix feed network for a switched multibeam antenna array," *TENCON 2009 - 2009 IEEE Region 10 Conference* , vol., no., pp.1-3, 23-26 Jan. 2009
- [13] Denidni, T.A.; Libar, T.E.; "Wide band four-port butler matrix for switched multibeam antenna arrays," *Personal, Indoor and Mobile Radio Communications*, 2003. *PIMRC 2003. 14th IEEE Proceedings on* , vol.3, no., pp. 2461- 2464 vol.3, 7-10 Sept. 2003
- [14] Jun Ouyang; , "A Circularly Polarized Switched-Beam Antenna Array," *Antennas and Wireless Propagation Letters*, *IEEE* , vol.10, no., pp.1325-1328, 2011
- [15] BAP50-03 General Purpose PIN Diode – NXP semiconductors, Available:www.nxp.com/documents/data_sheet/BAP50-03.pdf
- [16] M. Maqsood, S. Gao, T. Brown, M.Unwin, R. D. Steenwijk and J. D. Xu, "A Compact Multipath Mitigating Ground Plane for Multiband GNSS Antennas", *IEEE Transactions on Antennas and Propagation*, vol. 61, no. 5, pp 2775-2782, May 2013.
- [17] D. R. Jackson, J.T. Williams, Arun K. Bhattacharyya, Richard L. Smith, Stephen J. Buchheit and S.A. Long, "Microstrip Patch Designs That Do Not Excite Surface Waves," *IEEE Transactions on Antennas and Propagation*, vol. 41, pp. 1026-1037, Aug. 1993.
- [18] Young-Hoon Chun; Jia-Sheng Hong; , "Design of a compact broadband branch-line hybrid," *Microwave Symposium Digest, 2005 IEEE MTT-S International* , vol., no., pp. 4 pp., 12-17 June 2005.
- [19] John D. Kraus and Ronald J. Marhefka, "Antennas: For All Applications", 3rd Ed. McGraw Hill